Angiotensin AT_1 and AT_2 receptor heteromer expression in the hemilesioned rat model of Parkinson's disease that increases with levodopa-induced dyskinesia

Rafael Rivas-Santisteban (rrivasbioq@gmail.com)
Universitat de Barcelona https://orcid.org/0000-0002-2078-6819
Ana I. Rodriguez-Perez
Universidade de Santiago de Compostela
Ana Muñoz
Universidade de Santiago de Compostela
Irene Reyes-Resina
Universitat de Barcelona
José Luis Labandeira-García
Universidade de Santiago de Compostela
Gemma Navarro
Universitat de Barcelona
Rafael Franco
Universitat de Barcelona

Research

Keywords: Neuroinflammation, heteromer, G-protein-coupled receptor (GPCR), dyskinesia, levodopa

Posted Date: May 29th, 2020

DOI: https://doi.org/10.21203/rs.3.rs-18527/v2

Version of Record: A version of this preprint was published at Journal of Neuroinflammation on August 17th, 2020. See the published version at https://doi.org/10.1186/s12974-020-01908-z.

Abstract

Background/Aims: The renin-angiotensin system (RAS) is altered in Parkinson's disease (PD), a disease due to *substantia nigra* neurodegeneration and whose dopamine-replacement therapy, using the precursor levodopa, leads to dyskinesias as the main side effect. Angiotensin AT_1 and AT_2 receptors, mainly known for their role in regulating water homeostasis and blood pressure and able to form heterodimers ($AT_{1/2}$Hets), are present in the central nervous system. We assessed the functionality and expression of $AT_{1/2}$Hets in Parkinson Disease (PD).

Methods: Immunocytochemistry was used to analyze the colocalization between angiotensin receptors, bioluminescence resonance energy transfer was used to detect $AT_{1/2}$Hets. Calcium and cAMP determination, MAPK activation and label-free assays were performed to characterize signaling in homologous and heterologous systems. Proximity ligation assays was used to quantify receptor expression in mouse primary cultures and in rat striatal sections.

Results: We confirmed that AT_1 and AT_2 receptors form $AT_{1/2}$Hets that are expressed in cells of the central nervous system. $AT_{1/2}$Hets are novel functional units with particular signaling properties. Importantly, the coactivation of the two receptors in the heteromer reduces the signaling output of angiotensin. Remarkably, $AT_{1/2}$Hets that are expressed in both striatal neurons and microglia show a cross-potentiation, i.e. candesartan, the antagonist of AT_1 increases the effect of AT_2 receptor agonists. In addition, the level of striatal expression increased in the unilateral 6-OH-dopamine lesioned rat PD model and was markedly higher in parkinsonian-like animals that did not become dyskinetic upon levodopa chronic administration if compared with expression in those that became dyskinetic.

Conclusion: The results indicate that boosting the action of neuroprotective AT_2 receptors using an AT_1 receptor antagonist constitutes a promising therapeutic strategy in PD.

Introduction

The renin/angiotensin system (RAS) is composed of enzymes that produce angiotensin (Ang) peptides and of cell surface receptors that convey cytocrin signals to achieve specific cell responses. There are two angiotensin receptors (AT_1R and AT_2R) that belong to the superfamily of G-protein-coupled receptors. RAS has been abundantly studied in the periphery, mainly in relation with the control of arterial blood pressure. However, different laboratories have provided solid evidence on the relevant role of RAS in the central nervous system (CNS). Ang is an important regulator of motor control, and AT_1R and AT_2R have been suggested as targets to combat Parkinson's disease (PD) and related conditions such as levodopa (L-DOPA)-induced dyskinesias (Muñoz et al., 2014; Perez-Lloret et al., 2017).

Age is a main risk factor for sporadic PD, which is characterized by dysregulation of the dopaminergic function due to the death of dopaminergic neurons of the *substantia nigra* (SN). A local RAS has been reported in the SN (Garrido-Gil et al., 2013; Valenzuela et al., 2010), in which overactivity of AT_1R

correlates with aging-related alterations, neuronal death (Grammatopoulos et al., 2007; Labandeira-Garcia et al., 2013) and neuroinflammation (Jose L Labandeira-Garcia et al., 2017; Rodriguez-Perez et al., 2018). Microglial cells are the main mediators of neuroinflammation and despite once activated they are considered as detrimental, it is now known that they may undertake the pro-inflammatory (M1) or the neuroprotective (M2) phenotype. The search for pharmacological tools targeting G-protein-coupled receptors to convert M1 into M2 phenotype is an active field of research [9]. The role of AT_2R and the interplay between the two receptors in the above-mentioned changes due to Ang action in the aged or in the pathological brain is still unclear.

The cognate proteins for coupling to AT_1R and AT_2R are, respectively, Gq (also Gi) and Gi. Accordingly, agonists of AT_1R may mobilize calcium ion from intracellular stores, whereas agonists of AT_2R decrease the activity of adenylyl cyclase thus depressing the cAMP/PKA signaling (https://www.guidetopharmacology.org). Interestingly, the two receptors may interact, leading to the formation of receptor heteromers with particular properties: pharmacological, functional or both (Ferré et al., 2009; Porrello et al., 2011). On the one hand, heteromerization modifies receptor trafficking and ß-arrestin recruitment (Porrello et al., 2011). On the other hand, Ang II induces the formation of heteromers of the two receptors ($AT_{1/2}Hets$) in luminal membranes of kidney tubular epithelial LLC-PK1 cells. In these cells, the peptide activates a calcium channel, sarco/endoplasmic reticulum Ca^{2+}-ATPase (SERCA), that in kidney cells participates in the control of blood pressure (Ferrão et al., 2012).

The main target for pharmacological anti-parkinsonian interventions is the striatum that receives the SN dopaminergic input needed for motor control. What it is important is to know is whether AT_1 and AT_2 interact in the CNS, which is their physiological function and how their expression is alter in the course of a neurodegenerative disease. Accordingly, the aims of this paper were to i) get further insight into the properties of $AT_{1/2}Hets$ in a heterologous expression system, ii) investigate the expression and function of AT_1R, AT_2R and $AT_{1/2}Hets$ in striatal neurons and iii) investigate the expression and function of AT_1R, AT_2R and $AT_{1/2}Hets$ in striatal microglia in resting and activated states. The results show that AT_2R are expressed in neurons and in activated microglia where they interact with AT_1R to form $AT_{1/2}Hets$. Accordingly, a final aim was to discover differential expression of $AT_{1/2}Hets$ in striatal samples from parkinsonian and dyskinetic animals.

Materials And Methods

Reagents

Lipopolysaccharide (LPS), interferon-g (IFN-g) and forskolin were purchased from SigmaAldrich (St Louis, MO, USA), and Angiotensin II (Ang II), CGP-42112A (CGP), Candesartan (CAN) and PD123319 (PD) from Sigma-Aldrich (St Louis, MO).

HEK-293T cells and primary cultures

Human embryonic kidney (HEK-293T) cells were grown in Dulbecco's modified Eagle's medium (DMEM) (Gibco) supplemented with 2 mM L-glutamine, 100 µg/ml sodium pyruvate, 100 U/ml penicillin/streptomycin, MEM Non-Essential Amino Acids Solution (1/100) and 5% (v/v) heat inactivated Fetal Bovine Serum (FBS) (all supplements were from Invitrogen, Paisley, Scotland, UK).

To prepare mouse striatal primary microglial cultures, brain was removed from C57BL/6 mice of 2–4 days of age. Microglial cells were isolated following protocols described elsewhere (Newell et al., 2015; Pulido-Salgado et al., 2017; Saura et al., 2003) and grown in DMEM medium supplemented with 2 mM L-glutamine, 100 U/ml penicillin/streptomycin, MEM Non-Essential amino acids preparation (1/100) and 5% (v/v) heat inactivated Fetal Bovine Serum (FBS) (Invitrogen, Paisley, Scotland, UK). Briefly, striatum tissue was dissected, carefully stripped of its meninges and digested with 0.25% trypsin for 20 min at 37 ºC. The action of the proteolytic enzyme was stopped by adding an equal volume of culture medium (Dulbecco's modified Eagle medium-F-12 nutrient mixture, fetal bovine serum 10%, penicillin 100 U/mL, streptomycin 100 µg/mL and amphotericin B 0.5 µg/ml) with 160 µg/mL deoxyribonuclease I (all reagents from Invitrogen). Cells were brought to a single cell suspension by repeated pipetting followed by passage through a 100 µm-pore mesh and pelleted (7 min, 200 x g). Glial cells were resuspended in medium and seeded at a density of 3.5 x 10^5 cells/ml in 6-well plates for cyclic adenylic acid (cAMP) assays, in 12-well plates with coverslips for in situ proximity ligation assays (PLA) and in 96-well plates for mitogen-activated protein kinase (MAPK) activation experiments. Cultures were maintained at 37°C in humidified 5% CO_2 atmosphere and medium was replaced at DIV 2 and then once a week. At DIV 19-21 cells were treated with diluted trypsin (Saura et al., 2003) to obtain >98% pure microglial cultures.

For neuronal primary cultures, the striatum from mouse embryos (E19) was removed and the neurons were isolated as described by (Hradsky et al., 2013) and plated at a density of circa 120,000 cells/cm^2. The cells were grown in a neurobasal medium supplemented with 2 mM L-glutamine, 100 U/mL penicillin/streptomycin, and 2% (v/v) B27 supplement (Gibco) in a 6-, 12- or 96-well plate for 19-21 days. Cultures were maintained at 37ºC in humidified 5% CO_2 atmosphere and medium was replaced every 4–5 days.

Immunodetection of specific markers (Neu N for neurons and CD-11b for microglia) showed that neuronal preparations contained >98% neurons and microglia preparations contained, at least, 98% microglial cells (Navarro et al., 2018).

Parkinson's disease (PD) model generation, levodopa treatment and dyskinesia assessment

All experiments were carried out in accordance with EU directives (2010/63/EU and 86/609/CEE) and were approved by the Ethical committee of the University of Santiago de Compostela. Similar to the approach elsewhere described (Farré et al., 2015), an experimental design using male Wistar rats was aimed at obtaining four group of animals as described below. Animals were 8-week-old at the beginning of the experimental procedure.

Details of model generation, protocol of drug administration and behavioral analysis, performed by a blinded investigator, are given elsewhere (Muñoz et al., 2014; Pinna et al., 2014). Surgery was performed on rats anesthetized with ketamine/xylazine (1% ketamine -75 mg/kg-, and 2% xylazine -10- mg/kg). Lesions were produced in the right medial forebrain bundle to achieve complete lesion of the nigrostriatal pathway. The rats were injected with 12 µg of 6-hydroxy-DA (to provide 8 µg of 6-hydroxy-DA free base; SigmaAldrich) in 4 µl of sterile saline containing 0.2% ascorbic acid. These were considered “lesioned” animals. Injection of vehicle lead to generation of naïve (or non-lesioned) animals.

The 6-OH-dopamine hemilesioned rat is considered a PD model. Amphetamine-induced rotation was tested in a bank of eight automated rotometer bowls (Rota-count 8, Columbus Instruments, Columbus, OH, USA) by monitoring full (360°) body turns in either direction. Right and left full body turns were recorded over 90 min following an injection of D-amphetamine (2.5 mg/kg i.p.) dissolved in saline. Rats that displayed more than six full body turns/min ipsilateral to the lesion were included in the study (this rate would correspond to more than 90 % depletion of dopamine fibers in the striatum (Winkler et al., 2002).

Spontaneous use of forelimb can be measured by the cylinder test (Kirik et al., 2001; Schallert T, Kozlowski DA, Humm JL, 1997). Rats were placed individually in a glass cylinder (20 cm in diameter), and the number of left or right forepaw contacts were scored by an observer blinded to the animals’ identity and presented as left (impaired) touches in percentage of total touches. A control animal would thus receive an unbiased score of 50 %, whereas lesion usually reduces performance of the impaired paw to less than 20 % of total wall contacts.

Of the lesioned animals displaying parkinsonism-like behavior according to the above described tests (18 in total), 12 were chronically treated with L-DOPA daily for 3 weeks. A mixture of L-DOPA methyl ester (6 mg/kg) plus benserazide (10 mg/kg) was subcutaneously administered. The treatment reliably induces dyskinetic movements in some rats. As described in a previous report (Farré et al., 2015), abnormal involuntary movements were evaluated according to the rat dyskinesia scale described in detail elsewhere (Benito et al., 2003; De Filippis et al., 2009; Lee et al., 2000; Lundblad et al., 2002; Pinna et al., 2014). The severity of each AIM subtype (limb, orolingual, and axial) was assessed using scores from 0 to 4 (1, occasional, i.e., present <50% of the time; 2, frequent, i.e., present >50% of the time; 3, continuous, but interrupted by strong sensory stimuli; 4, continuous, not interrupted by strong sensory stimuli). Rats were classified as “dyskinetic” if they displayed a ³ 2 score per monitoring period on at least two abnormal involuntary movement (AIM) subtypes. Animals classified as “non-dyskinetic” exhibited either no L-DOPA-induced abnormal involuntary movements or very mild/occasional ones (Ohlin et al., 2012). Animals with low scores, i.e., either non-dyskinetic or dyskinetic, were discarded. In summary four groups of animals were obtained: i) non-lesioned, ii) lesioned treated with vehicle iii) lesioned L-DOPA-treated becoming dyskinetic and iv) lesioned that upon L-DOPA-treatment did not become dyskinetic. In every animal tyrosine hydroxylase immunostaining was performed in sections taken post-mortem (Garrido-Gil et al., 2017; Muñoz et al., 2014); selected animals undergoing 6-OH-dopamine treatment showed in the lesioned hemisphere a >95% nigral dopaminergic denervation. Overall 4 animals, those with better scores,

were selected in each of following 4 groups: naïve, lesioned, lesioned/L-DOPA dyskinetic and lesioned/L-DOPA non dyskinetic. PLA analysis (see below) was performed in different fields of striatal sections from each of the 16 finally selected animals. The striatum was delimited in sections using a bright field and images were captured within delimitation coordinates.

Fusion proteins

Human cDNAs for AT_1, AT_2 and s_1 receptors cloned into pcDNA3.1 were amplified without their stop codons using sense and antisense primers harboring either BamHI and HindIII restriction sites to amplify AT_1R and AT_2R or BamHI and EcoRI restriction sites to amplify s_1 receptor. Amplified fragments were then subcloned to be in frame with an enhanced yellow fluorescent protein (pEYFP-N1; Clontech, Heidelberg, Germany) or a Rluc (pRluc-N1; PerkinElmer, Wellesley, MA) on the C-terminal end of the receptor to produce AT_1R-YFP, AT_2R-RLuc, AT_2R-YFP and s_1R-RLuc fusion proteins.

Cell transfection

HEK-293T cells were transiently transfected with the corresponding cDNA by the PEI (PolyEthylenImine, SigmaAldrich, St. Louis, MO) method (Franco et al., 2019; Hinz et al., 2018). Briefly, the corresponding cDNA diluted in 150 mM NaCl was mixed with PEI (5.5 mM in nitrogen residues) also prepared in 150 mM NaCl for 10 min. The cDNA-PEI complexes were transferred to HEK-293T cells and were incubated for 4 hours in a serum-starved medium. Then, the medium was replaced by fresh supplemented culture medium and cells were maintained at 37 ºC in a humid atmosphere of 5% CO_2. 48 hours after transfection, cells were washed, detached, and resuspended in the assay buffer.

Immunocytochemistry

HEK-293T cells were seeded on glass coverslips in 12-well plates. On DIV 2, cells were transfected with AT_1R-YFP cDNA (1 µg), AT_2R-Rluc cDNA (1 µg) or both. On DIV 4, cells were fixed in 4% paraformaldehyde for 15 min and washed twice with PBS containing 20 mM glycine before permeabilization with PBS-glycine containing 0.2% Triton X-100 (5 min incubation). Cells were blocked during 1 hour with PBS containing 1% bovine serum albumin. HEK-293T cells were labeled with a mouse anti-Rluc antibody (1/100; Millipore, Darmstadt, Germany) and subsequently treated with Cy3 conjugated anti-mouse (1/200; Jackson ImmunoResearch (red)) IgG (1 hour each). The AT_1R-YFP expression was detected by YFP´s own fluorescence. Controls using untransfected cells and cells incubated without the primary antibody are shown in Supplementary Figure S1. Samples were washed several times and mounted with 30% Mowiol (Calbiochem). Images were obtained in a Leica SP2 confocal microscope (Leica Microsystems) with the 63X oil objective.

Bioluminescence resonance energy transfer (BRET) assays

For BRET assays, HEK-293T cells were transiently cotransfected with a constant amount of cDNA encoding for AT_2R-RLuc (0.9 µg) and with increasing amounts of cDNA corresponding to AT_1R-YFP (0.5

to 4 µg). For negative control, HEK-293T cells were transiently cotransfected with a constant amount of cDNA encoding for s_1-RLuc (0.75 µg) and with increasing amounts of cDNA corresponding to AT_2R-YFP (0.1 to 4 µg). To control the cell number, sample protein concentration was determined using a Bradford assay kit (Bio-Rad, Munich, Germany) using bovine serum albumin (BSA) dilutions to prepare the standard absorbance versus concentration relationship. To quantify fluorescent proteins, cells (20 µg protein) were distributed in 96-well microplates (black plates with a transparent bottom) and fluorescence was read in a Fluostar Optima Fluorimeter (BMG Labtech, Offenburg, Germany) equipped with a high-energy xenon flash lamp, using a 10 nm bandwidth excitation filter at 485 nm. For BRET measurements, the equivalent of 20 µg of cell suspension was distributed in 96-well white microplates with white bottom (Corning 3600, Corning, NY) and 5 µM coelenterazine H (Molecular Probes, Eugene, OR) was added. One minute after adding coelenterazine H, BRET was determined using a Mithras LB 940 reader (Berthold Technologies, DLReady, Germany), which allows the integration of the signals detected in the short-wavelength filter at 485 nm and the long-wavelength filter at 530 nm. To quantify AT_2R-RLuc expression, luminescence readings were performed 10 minutes after the addition of 5 µM coelenterazine H. MilliBRET units (mBU) are defined as:

See formula 1 in the supplementary files.

where C_f corresponds to [(long-wavelength emission)/(short-wavelength emission)] for the RLuc construct expressed alone in the same experiment.

Detection of cytoplasmic calcium ion

HEK-293T cells were cotransfected with the cDNA for the Ang receptors AT_1 (1 µg) and/or AT_2 (1 µg) and the GCaMP6 calcium sensor (1 µg) (Chen et al., 2013) by the use of PEI method (Section “Cell Transfection”). 48 hours post-transfection, HEK-293T cells plated in 6-well black, clear bottom plates, were incubated with Mg^{2+}-free Locke’s buffer (154 mM NaCl, 5.6 mM KCl, 3.6 mM $NaHCO_3$, 2.3 mM $CaCl_2$, 5.6 mM glucose, 5 mM HEPES, pH 7.4) supplemented with 10 µM glycine. Receptor antagonists were added only 15 min before readings to allow efficient binding to receptors while avoiding unspecific or long-term noxious events. Receptor agonists were added right before readings as calcium level increase when mediated by Gq-coupled receptors is very quick. Fluorescence emission intensity of GCaMP6 was recorded at 515 nm upon excitation at 488 nm on the EnSpire® Multimode Plate Reader for 150 s every 5 s at 100 flashes per well.

cAMP level determination

The analysis of cAMP levels was performed in HEK-293T cells transfected with cDNA for AT_1 (1 µg) and/or AT_2 (1 µg) receptors in primary cultures of striatal neurons or glia using the Lance Ultra cAMP kit (PerkinElmer). The optimal cell density to obtain an appropriate fluorescent signal was first established by measuring the TR-FRET signal as a function of forskolin concentration using different cell densities. Forskolin dose-response curves were related to the cAMP standard curve in order to establish which cell

density provides a response that covers most of the dynamic range of cAMP standard curve. 2 hours before the experiment the medium was substituted by serum-starved DMEM medium. Cells (2,000 HEK-293T cells, 4,000 striatal neurons or glial cells by well in 384-well microplates) growing in medium containing 50 µM zardaverine were pre-treated with the AT_1R or AT_2R antagonists (Candesartan and PD123319 respectively) or the corresponding vehicle at 24°C for 15 min, and stimulated with the AT_1R and/or AT_2R agonists (Ang II and CGP-42112A respectively) for 15 min before adding 0.5 µM forskolin or vehicle, and incubating for an additional 15 min period. After 1 hour, fluorescence at 665 nm was analyzed on a PHERAstar Flagship microplate reader equipped with an HTRF optical module (BMG Labtech). A standard curve for cAMP was obtained in each experiment.

Extracellular signal-regulated kinases 1/2 (ERK1/2) phosphorylation

To determine ERK1/2 phosphorylation, 40,000 HEK-293T cells transfected with cDNA for AT_1R (1 µg) and/or AT_2R (1 µg) or 50,000 striatal neurons or glial cells primary cultures were plated in each well of transparent Deltalab 96-well microplates. Two hours before the experiment, the medium was substituted by serum-starved DMEM medium. Then, cells were treated or not for 15 min with the selective antagonists Candesartan or PD123319 in serum starved DMEM medium followed by 7 min treatment with the selective agonists Ang II and/or CGP-42112A. Cells were then washed twice with cold PBS before the addition of lysis buffer (15 min treatment). 10 µL of each supernatant were placed in white ProxiPlate 384-well microplates and ERK1/2 phosphorylation was determined using AlphaScreen®SureFire® kit (Perkin Elmer) following the instructions of the supplier and using an EnSpire® Multimode Plate Reader (PerkinElmer, Waltham, MA, USA).

Dynamic Mass-Redistribution (DMR) label free assays

Cell signaling was explored using an EnSpire® Multimode Plate Reader (PerkinElmer, Waltham, MA, USA) by a label-free technology. Cellular cytoskeleton redistribution movement induced upon receptor activation were detected by illuminating the underside of the plate with polychromatic light and measured as changes in wavelength of the reflected monochromatic light that is a sensitive function of the index of refraction. The magnitude of this wavelength shift (in picometers) is directly proportional to the amount of DMR. To determine the label free-DMR signal, 10,000 HEK-293T cells transfected with cDNA for AT_1R (1 µg) and/or AT_2R (1 µg) receptors or 10,000 striatal neurons or glial cells primary cultures were plated on each well of transparent 384-well fibronectin coated microplates to obtain 70-80% confluent monolayers, and kept in the incubator for 24 h. Previous to the assay, cells were washed twice with assay buffer (HBSS with 20 mM HEPES, pH 7.15, 0.1% DMSO) and incubated in the reader for 2 hours in 30 µl/well of assay-buffer at 24°C. Hereafter, the sensor plate was scanned and a baseline optical signature was recorded for 10 minutes before adding 10 µl of antagonists (Candesartan or PD123319) dissolved in assay buffer, followed by the addition, 30 min later of 10 µl of selective agonists (Ang II and/or CGP-42112A) also dissolved in assay buffer. DMR responses induced by the agonist were monitored for a minimum of 3,600 s.

Proximity Ligation Assay (PLA)

Detection in natural sources of clusters formed by AT_1 and AT_2 receptors was addressed in striatal neurons, primary cultures of glial cells and rat brain sections.

Rats were processed for histological analysis as it follows. Animals were injected an overdose of chloral hydrate and transcardial perfusion fixation quickly undertaken using cold 4% paraformaldehyde in 0.1 M phosphate buffer (PB), pH 7.4. Brains were removed, washed and cryoprotected in the same buffer containing 20% sucrose. Serial 40 µm thick coronal sections were then cut with a freezing microtome and those containing the striatum were collected in cryoprotectant solution.

Cells were grown on glass coverslips, fixed in 4% paraformaldehyde for 15 min, washed with PBS containing 20 mM glycine to quench the aldehyde groups, permeabilized with the same buffer containing 0.05% Triton X-100 for 5 to 15 min and washed with PBS.

Cells and sections were then similarly processed. After 1 hour incubation at 37°C with the blocking solution in a pre-heated humidity chamber, samples were incubated overnight at 4ºC with a mixture of a mouse monoclonal anti-AT_1R antibody (1/100, sc-515884, Santa Cruz Biotechnology, Texas, USA), a rabbit monoclonal anti-AT_2R antibody (1/100, ab92445, Abcam, Cambridge, UK) and Hoechst (1/100 from stock 1 mg/mL; SigmaAldrich) to stain the nuclei. The antibodies were validated following the method in the technical brochure of the vendor with fairly similar results and also by immunofluorescence in HEK-293T cells (transfected versus untransfected). Samples from KO animals were not available for validation.

Cells or brain sections were further processed using the PLA probes detecting primary antibodies (Duolink In Situ PLA probe Anti-Mouse plus and Duolink In Situ PLA probe Anti-Rabbit minus) (1/5 v:v for 1-hour at 37ºC). Ligation and amplification were done as indicated by the supplier (SigmaAldrich) and cells were mounted using the mounting medium 30% Mowiol (Calbiochem). To detect red dots corresponding to $AT_{1/2}$Hets, samples were observed in a Leica SP2 confocal microscope (Leica Microsystems, Mannheim, Germany) equipped with an apochromatic 63X oil-immersion objective (N.A. 1.4), and a 405 nm and 561 nm laser lines. For each field of view a stack of two channels (one per staining) and 3 Z-planes with a step size of 1 µm were acquired. The Andy's Algorithm (Law et al., 2017), a specific ImageJ macro for reproducible and high-throughput quantification of the total PLA foci dots and total nuclei, was used for data analysis.

Statistical analysis

The data in graphs are the mean ± SEM. GraphPad Prism software version 7 (San Diego, CA, USA) was used for data fitting and statistical analysis. The test of Kolmogorov-Smirnov with the correction of Lilliefors was used to evaluate normal distribution and the test of Levene to evaluate the homogeneity of variance. The Student's t test and one way ANOVA were used for comparing, respectively, two or >2

means. When indicated, Bonferroni's method was used as a *post-hoc* test for multiple comparisons. Significant differences were considered when the p value was <0.05.

Results

Functionality of $AT_{1/2}$Hets in a heterologous expression system

Interactions between AT_1 and AT_2 receptors have been previously reported (Ferrão et al., 2012; Porrello et al., 2011). Hence, we first investigated whether in HEK-293T cells and in our assay conditions AT_1 and AT_2 receptors may form heteromers. We analyzed the colocalization of angiotensin receptors at the plasma membrane by using HEK-293T cells coexpressing AT_1R and AT_2R fused to, respectively, the yellow fluorescent protein (YFP) and Renilla luciferase (Rluc). The proper traffic of fusion proteins to the cell membrane was confirmed by immunocytochemical analysis (Fig 1A-B). The high degree of colocalization between AT_1R-YFP and AT_2R-Rluc in the plasma membrane and in the cytosol is shown in yellow (Fig 1C). To know whether a direct interaction between AT_1 and AT_2 receptors is possible, BRET assays were performed in HEK-293T cells expressing a constant amount of a fusion protein consisting of AT_2R and Renilla Luciferase (AT_2R-Rluc) and increasing amounts of AT_1R fused to YFP (AT_1R-YFP). The saturation curve in Fig. 1D indicates close proximity between the two Ang receptors. The $BRET_{max}$ and $BRET_{50}$ values were 42 ± 1 mBU and 6 ± 2, respectively. When HEK-293T cells were transfected with a constant amount of cDNA for s1-Rluc and increasing amounts of cDNA for AT_1R-YFP, a linear response was observed indicating a nonspecific interaction of this negative control (Fig. 1D). These results confirm that the two Ang receptors may form heteromers in living HEK-293T cells. The proper functionality of fusion proteins was confirmed by cAMP assays (data not shown). A schematic representation of the technique is shown in Fig. 1E.

To characterize the $AT_{1/2}$Het functionality, signaling assays were performed in single-transfected HEK-293T cells and in cotransfected $AT_{1/2}$Hets-expressing cells. Cytosolic calcium levels, cAMP determination, ERK1/2 phosphorylation and label-free DMR assays were performed after treatment with AT_1R and/or AT_2R ligands. Consistent with Gq coupling of AT_1R, treatment of AT_1R-expressing cells with Ang II led to a marked increase in cytosolic calcium levels. The effect was receptor-mediated, as it was blocked by candesartan, the AT_1R antagonist (Fig. 2A). In AT_2R expressing cells, the AT_2R agonist CGP-42112A did not induce mobilization of the ion. These results agree with AT_2R not engaging Gq proteins. In cotransfected cells, CGP-42112A did not produce any effect but reduced the response peak produced by Ang II. Hence, within the $AT_{1/2}$Het, AT_2R stimulation inhibits the AT_1 receptor signaling. Unlike the selective AT_1R antagonist, candesartan, which blunted the agonist effect, the selective AT_2R antagonist, PD123319, potentiated the AT_1R-mediated effect (Fig. 2C).

Consistent with AT_2R coupling to Gi, CGP-42112A reduced the forskolin-induced cAMP cytosolic levels in AT_2R single transfected cells. Interestingly, in AT_1R expressing cells, Ang II treatment also reduced the

forskolin-induced cAMP levels. These effects can be explained by AT_1R coupling not only to Gq, but also to Gi proteins. These effects were receptor-mediated and specific as they were blocked by the corresponding antagonist (Fig. 2D-E). Analysis of cAMP-PKA signaling in cotransfected cells is more complex. On the one hand, all agonists reduced forskolin-induced [cAMP] and each antagonist blocked the effect of the corresponding agonist. Simultaneous administration of Ang II and CGP-42112A did not result in an additive effect. On the other hand, the antagonist of the AT_2R enhanced the effect induced by the AT_1R agonist and *vice-versa,* the antagonist of the AT_1R enhanced the effect of the AT_2R agonist (Fig. 2F). These latter results fit with data from calcium release experiments assays where the antagonist of the AT_2R potentiated the action of Ang II. Then, it seems that both angiotensin receptors regulate one another via heteromerization. The negative regulation can be reversed and the antagonist of one receptor can even reinforce the output due to activation of the partner receptor.

In AT_1R-expressing cells a marked increase in agonist-induced ERK1/2 phosphorylation that was blocked by candesartan was observed, while in AT_2R-expressing cells a mild non-significant effect was obtained by treatment with the agonist, CGP-42112A (Fig. 3A-B). Remarkably, $AT_{1/2}$Hets expression in cotransfected cells led to a significant increase in ERK1/2 phosphorylation upon Ang II treatment. The selective AT_2R agonist was still unable to produce any significant effect but, in combined treatments, it markedly reduced the effect induced by Ang II (Fig. 3C). Therefore, these results are in the same line with that observed in calcium release and cAMP accumulation, indicating that both receptors inhibit one another in the $AT_{1/2}$Het.

DMR was modified by agonists in both types of single-transfected cells. In AT_1R-expressing cells the antagonist could not revert totally the effect of the agonist, indicating that part of the output signal is due to off-site action of Ang II (Fig. 3D). In contrast, the effect of CGP-42112A on AT_2R-expressing was totally blocked by PD123319 (Fig. 3E). In cotransfected cells, the results indicate that both angiotensin receptors show a characteristic signal that is blocked by selective antagonists. However, coactivation in these cells produced an important decrease in the signal. This effect is named negative crosstalk and it is similar to that observed in MAPK phosphorylation assays (Fig. 3E). The enhancement by candesartan of the effect of CGP-42112A, the AT_2R agonist, was also noticed.

In summary, these results indicate a particular functionality of the $AT_{1/2}$Het, namely Ang is able to engage two different signaling pathways. This dual effect is regulated by activation of the partner receptor within the $AT_{1/2}$Het as i) activation of AT_1R blocks AT_2R agonist induced effect and *vice-versa* and ii) AT_1R antagonist releases the inhibition exerted by AT_2R over AT_1R and *vice-versa*.

Functionality of AT_1R and AT_2R in primary cultures of striatal neurons

On the basis of the above-described relevance of Ang receptors in motor control and as potential targets to combat PD, we investigated Ang receptor-mediated signaling in primary cultures of neurons isolated from mouse striatum. Reduction of forskolin-induced [cAMP] increases were obtained using Ang II, while

no sign of Gi-coupled AT_2R was detectable (Fig. 4A). Interestingly, in simultaneous treatment with agonists, a lower decrease of forskolin-induced [cAMP] indicated the presence of AT_2R whose activation reduced AT_2R-mediated signaling. In the presence of the AT_1R antagonist, candesartan, the AT_2R agonist, CGP-42112A, induced a significant decrease in forskolin-induced cAMP levels. These results indicate that in the $AT_{1/2}$ Het, the AT_2R signal is inhibited by AT_1R expression and this effect is counteracted by AT_1R antagonists. Similar results were confirmed in experiments of ERK1/2 phosphorylation determination in cultured striatal neurons, where cells responded (moderately) to Ang II and non-significantly to CGP-42112A (Fig. 4B). However, candesartan pretreatment potentiated AT_2R signal. In agreement with the results in HEK-293T cells, cotreatment with agonists induced a lower signal to that induced by angiotensin II, indicating a negative crosstalk effect in both cAMP and MAPK phosphorylation signaling pathways. Overall, these cells express $AT_{1/2}$Hets with similar functional characteristics to that observed in cotransfected HEK-293T cells.

Functionality of AT_1R and AT_2R in primary cultures of striatal microglia. Expression of $AT_{1/2}$Hets.

Before assessing the functionality of Ang receptors in resting and LPS+IFNg activated microglia isolated from striatum, we used in situ PLA to assess the expression of $AT_{1/2}$Hets; PLA is instrumental to detect clusters of interacting proteins in natural sources. Fig. 5B shows that resting cells have a few number of red dots due to $AT_{1/2}$Hets, while the negative control show a negligible number of red dots (Fig. 5A). Interestingly, the red label was markedly increased in activated cells, as shown in Fig. 5C and in the bar graph of Fig. 5D indicating that $AT_{1/2}$Hets expression increases in activated microglia. We then performed cAMP level determination and ERK1/2 phosphorylation assays in resting and activated microglial cells. The functionality of AT_1R, AT_2R and/or $AT_{1/2}$Hets in resting cells was very low. But in cAMP assays, pretreatment with candesartan potentiated AT_2R induced signaling, and PD123319 potentiated AT_1R functionality (Fig. 5E, G). In contrast, the angiotensin-receptor-mediated signaling was more robust in LPS+IFNg activated cells (Fig. 5F, H). In cAMP assays, the agonist of the two receptors reduced the forskolin-induced levels of this second messenger, although receptor costimulation did not lead to any additive effect. As it occurred in HEK-293T cells and neuronal primary cultures, antagonist pretreatments potentiated the partner receptor signal. On the other hand, the agonist of any of the two receptors activated the MAPK signaling pathway, while simultaneous stimulation completely blunted the ERK1/2 phosphorylation effect in activated microglia. In this signaling pathway antagonists blocked the cognate receptor and did not potentiate the activation of the partner receptor in the heteromer. Taken together, these results indicate that $AT_{1/2}$Hets are significantly expressed in activated microglia showing the same properties than those displayed in heterologous system.

Expression $AT_{1/2}$Hets in the striatum of parkinsonian and dyskinetic rats.

Striatal sections of naïve and of 6-OH-dopamine hemilesioned rats, treated or not with L-DOPA and divided into L-DOPA/dyskinetic or resistant to L-DOPA-induced dyskinesia were prepared as described in methods. PLA assays were performed simultaneously and in identical conditions to detect the occurrence

and the amount of $AT_{1/2}$Hets. A representative image of each of the conditions is shown in Fig. 6A-D, while quantitation is shown in the form of bar graph in Fig. 6E. Whereas the amount of $AT_{1/2}$Hets was negligible in the non-lesioned striatum, the lesioned one displayed more receptor clusters. L-DOPA/dyskinetic animals showed a two-fold increase if compared with the ipsilateral hemisphere of lesioned rats. Remarkably, animals resistant to L-DOPA-induced dyskinesia had a circa 10-fold increase in the amount of $AT_{1/2}$Hets (compared to control, non-lesioned hemisphere). These results show that, in this specific PD model, of maximal dopaminergic denervation similar to that observed in advanced stages of the disease there is striatal expression of the heteromer that is increased upon L-DOPA administration. Remarkably, a much higher increase in expression was found in L-DOPA-treated animals that did not become dyskinetic. The increase is evident in cells with larger nuclei, likely neurons, and in cells with smaller nuclei, likely glia.

Discussion

Details of peripheral RAS have been instrumental to develop a successful therapy to combat hypertension. The knowledge of RAS in the CNS is still fragmentary but with repercussions in dopaminergic neurotransmission and potential in PD and/or PD therapy-related dyskinesias. One of the added value of any future PD intervention based in central RAS is the safety of angiotensin receptor antagonists that have been used for decades in hypertensive patients. While no double-blind placebo controlled clinical trials have been designed, epidemiological studies addressing the risk of hypertensive patients taking angiotensin receptor antagonists have been performed. The fact that not all the drugs are able to cross the blood-brain barrier complicates data analysis. Anyhow, some of the reported results appear promising and using ß-blockers as a control and 65001 hypertensive patients for >4 years (Lee et al., 2014) showed that the use of certain antihypertensives (angiotensin receptor blockers included) associates with reduced PD risk. The still unsolved question is whether such drugs may be of benefit in improving symptoms, avoiding L-DOPA-induced dyskinesias and/or in delaying the progression of the disease.

First of all, it has been described that the global effects of angiotensin on AT_1 and AT_2 receptors are opposite. In several tissues overactivity of the AT_1 receptor has been linked to aging-related pro-inflammatory changes (Franceschi et al., 2006; Labandeira-Garcia et al., 2017). Different mechanisms have been proposed to explain counteracting effects of AT_2R on AT_1R signaling (see (Padia and Carey, 2013; Patel and Hussain, 2018; Steckelings et al., 2005) for review). Although the issue is complex, the expression of AT_2R in brain suggests a relevant role in the regulation of neuroinflammation. On the one hand, as earlier indicated, the two angiotensin receptors may interact leading to receptor heteromers with particular properties such as regulating SERCA activity (Ferrão et al., 2012; Porrello et al., 2011). On the other hand, several heteromers formed by angiotensin receptors have been described. Among other examples, (Siddiquee et al., 2013) it has been reported that apelin and AT_1 receptors interact and that the resulting heteromers mediate the apelin inhibition of AT_1R-mediated actions. MAS protooncogene, the novel player in AT research, rescues a defective AT_1R, likely by forming heterodimers (Santos et al., 2007).

The discovery of interaction between AT_1R and the most abundant receptor in the CNS, namely the cannabinoid CB_1 receptor, has led to hypothesize that these functional units may lead to pathogenic actions when AT is produced. However, the potential toxicity was studied in hepatic cells in relation to ethanol consumption but it was not assayed in neuronal cell models (Rozenfeld et al., 2011). The AT_1R may form complexes with a variety of adrenergic receptors (Barki-Harrington et al., 2003; González-Hernández et al., 2010) although their relevance to CNS physiology seems scarce. Less data are available for the AT_2R receptor that may interact (in the periphery) with MAS and with bradykinin B2 receptors (Abadir et al., 2006; Leonhardt et al., 2017; Patel and Hussain, 2018; Villela et al., 2015). In addition, $AT_{1/2}$Hets may form dimers that, may eventually interact with MAS or with bradykinin B2 receptors in cells in which three of these receptors are expressed together (Cerrato et al., 2016; Rubio-Ruíz et al., 2014). One of the relevant results in this study is the demonstration in a rat model of microglial $AT_{1/2}$Hets expression and its upregulation correlating with PD and with ulterior treatment with L-DOPA, the most extended therapeutic agent in PD (Birkmayer and Hornykiewicz, 1964; Hornykiewicz, 2006; Olanow et al., 2004).

What is relevant for PD pathophysiology and disease progression is to delay the death of the approximately 30% nigral dopaminergic neurons that are left at the time of PD diagnosis. Glia in general, and microglia in what concerns to neuroinflammation, are key to preserve neurons from death. AT_1Rs have been proposed as targets to reduce chronic neuroinflammation (Jarrott and Williams, 2016; Joglar et al., 2009; Rodriguez-Pallares et al., 2008) as that occurring in PD. The general idea is that activation of the AT_1R is detrimental, for instance by a microglia-mediated enhancement of neuronal loss in status epilepticus induced in rats (Sun et al., 2015). In a previous study performed in the SN of rats we showed that angiotensin-induced Rho-kinase activation was involved in NADPH-oxidase activation, which, in turn, was involved in angiotensin-induced Rho-kinase activation (Rodriguez-Perez et al., 2015). In addition, a prevention of astrocyte activation and promotion of hippocampal neurogenesis has been attributed to AT_1R blockade and subsequent prevention of NFκB and MAP kinase signaling and activation of Wnt/β-catenin signaling (Bhat et al., 2018). In our experimental conditions performed with already activated striatal microglia, MAP kinase signaling is suppressed by combined treatment with AT_1 and AT_2 receptor agonists. In the retina, AT_1R activation results in regulating microglial activation thus suggesting that AT may have important implications in diabetic retinopathy (Phipps et al., 2018). To our knowledge the expression of $AT_{1/2}$Hets in retinal cells has not been addressed yet. In agreement with the occurrence of a RAS opposite arm consisting of AT_2R (also of Mas receptor) (JL Labandeira-Garcia et al., 2017), AT_2R activation attenuates microglial activation in an autoimmune encephalomyelitis rodent model (Valero-Esquitino et al., 2015). Activation of the receptor is neuroprotective in a model of ischemia induced in conscious rats (McCarthy et al., 2014). Similarly, the report by Bennion et al. (Bennion et al., 2017) proves that AT_2R activation in neurons and glial cells affords long-term neuroprotection in stroke, by both direct and indirect mechanisms. Recent studies show that the receptor prevents/attenuates pro-inflammatory microglial activity via protein phosphatase 2A-mediated inhibition of protein kinase C (Bhat et al., 2019).

To our knowledge the AT_1-bradikinin B2 heteroreceptor complex was the first to be associated to a peripheral-affecting disease. In fact the expression of the heteromer was increased thus mediating a higher Ang responsiveness in preeclampsia, a disease that markedly alters blood pressure in pregnancy (AbdAlla et al., 2001). The heteromer physiological function involves diverse signaling pathways and a variety of cells events such as phosphorylation of c-Jun terminal kinase and enhanced production of nitric oxide and a second messenger, cGMP (Abadir et al., 2006). An unbalanced proportion of AT_1-bradikinin B2 receptor heteromers alters activation of cognate G-proteins and receptor desensitization (AbdAlla et al., 2000; Wilson et al., 2013). We have collected data on differential expression of dopamine-receptor-containing heteromers in PD and the conclusion is that very often the expression of heteromers is altered in one or different stages of the disease. Usually the expression of those heteromers in dyskinesia is lower than in PD animals treated with L-DOPA but not displaying dyskinesias. Hence, this is the first example in which the already enhanced expression of heteromers in parkinsonian conditions is further increased in animals that were not rendered dyskinetic by L-DOPA treatment. These results are relevant as antagonists of angiotensin are considered as having potential to both improve PD symptoms and minimize L-DOPA-induced dyskinesias.

As in any other study focused on a neurodegenerative disease, there are a number of limitations. Among them we are extrapolating to “adult” cells using primary cells obtained from fetuses of neonates. Although this is a common procedure because the procedure of isolation of primary neural cells from adult animals are not optimized, a note of caution is needed. Another limitation of our study is the variety of neural cell types. It is a challenge to know the relative expression of receptors in projection neurons, in choline acetyltransferase (ChAT), parvalbumin (PV), calretinin (CR) or nitric oxide synthase interneurons and in astroglia and microglia, which may be at different degrees of activation depending on the disease status. Furthermore, receptor functionality in response to a given receptor ligand may vary from cell to cell (Franco et al., 2018) and at onset of disease when comparing naïve versus L-DOPA-treated individuals.

But in any case, pharmacological manipulation of RAS components presents potential in PD (JL Labandeira-Garcia et al., 2017). One of the relevant findings in this paper is the insensitivity of AT_2R to agonist treatment of striatal neurons. Indeed those neurons express both Ang receptor types as previously demonstrated (Garrido-Gil et al., 2017). However, it is more remarkable that it becomes functional in the presence of candesartan. There are few examples of similar findings and a recent one consists of progressive decrease of adenosine A_{2A} receptor functionality upon coexpression of another adenosine receptor, A_{2B}, and formation of A_{2A}/A_{2B} heteroreceptor complexes. This phenomenon is due to allosteric inter-protomer interactions in the heteromer, i.e. the presence of one receptor blocks the signaling of the partner receptor in the complex (Hinz et al., 2018). Interestingly, the presence of an antagonist could make, as in the case of Ang receptor heteromers in striatal neurons, appear AT_2R functionality back. Therefore, AT_1R antagonists in these neurons may achieve two benefits, which are repressing the detrimental actions mediated by the AT_1R while making that the AT_2R becomes functional and provides the benefits associated to its activation. Furthermore, in terms of looking for interventions to

prevent PD disease progression there is enough information to agree that microglial cells may be key if there is a way to skew the physiology to acquire the M2 neuroprotective phenotype. On the one hand, neuronal alpha-synuclein produces an upregulation of AT_1R while increasing in microglia the proportion of pro-inflammatory M1 versus neuroprotective M2 markers; accordingly it is suggested that antagonists already used in hypertension and able to cross the blood-brain barrier, may be repurposed for the therapy of PD (Rodriguez-Perez et al., 2018). On the other hand, microglial AT_2Rs, constituent in $AT_{1/2}Hets$, show promise as i) they are upregulated in both parkinsonian conditions and in L-DOPA-induced dyskinesias and ii) their activation is seemingly neuroprotective. Remarkably, $AT_{1/2}Hets$ do not show cross-antagonism, a property displayed by many heteromers and that would lead to a therapeutic dead end in terms of neuroprotection; instead the antagonist of one receptor releases the brake on activation of the partner receptor. Taken together, the opposite action of AT_1 and AT_2 receptors, their expression in microglia and the marked upregulation of $AT_{1/2}Hets$ lacking cross-antagonism but displaying antagonist-mediated cross-potentiation, suggest that interventions aimed at antagonizing central AT_1Rs to potentiate AT_2R-mediated actions may be beneficial in PD.

Conclusions

Main conclusions

The present study demonstrates that AT_1 and AT_2 receptors form $AT_1/_2Hets$ that are expressed in cells of the central nervous system. $AT_1/_2Hets$ are novel functional units with particular signaling properties. Importantly, the coactivation of the two receptors in the heteromer reduces the signaling output of angiotensin. Remarkably, $AT_1/_2Hets$, which are expressed in both striatal neurons and microglia, show a cross-potentiation, i.e. candesartan, the antagonist of AT_1 increases the effect of AT_2 receptor agonists. In addition, the level of expression in the unilateral 6-OH-dopamine lesioned rat PD model increases upon L-DOPA treatment and is maximal in those animals that do not become dyskinetic.

Importance and relevance of the study reported

These findings reported are potentially important because they indicate that boosting the action of neuroprotective AT_2 receptors using an AT_1 receptor antagonist constitutes a promising therapeutic strategy in PD. The strategy may consist of designing AT_1R receptor antagonists able to readily cross the blood-brain barrier and effective in releasing the brake on the AT_2 receptor. The fact that SARS-CoV-2 uses angiotensin converting enzyme 2 (ACE2) as receptor, that ACE2 interacts with angiotensin receptors, that some COVID-19 patients with severe symptoms display a “cytokine storm” driven by macrophages and/or suffer neurological alterations, adds interest to the present work on the RAS system in microglia.

Declarations

Ethics Approval and consent to participate

All animal experiments were carried out in accordance with EU directives (2010/63/EU and 86/609/CEE) and were approved by the Ethical committee of the University of Santiago de Compostela (#2016/0345) whose resolutions are supervised by regional and National regulatory bodies.

Declarations

Consent for publication

Co-authors have acknowledged reception of the final version of the manuscript and concur with the submission

Availability of data and material

All data are available upon request to the corresponding author(s)

Competing interests

Author declares no conflict of interest

Funding

This work was supported by grants of the Spanish Ministry of Health (PI17/00828 and CIBERNED) and from the Spanish Ministry of Science, Innovation and Universities (RTI2018-098830-B-I00 and RTI2018-094204-B-I00; they include EU FEDER funds).

Authors' contributions

RF, GN and JLL designed, supervised the work in the different laboratories and validated the data in the manuscript. RRS and IRR performed biophysical, signaling and immunohistochemical assays. RRS analyzed proximity ligation assay data. AM and AIRP did the lesions, characterized the different animal groups and prepared brain sections. RF wrote the first draft that was edited first by GN and JLL and, subsequently, by all co-authors.

Acknowledgements

We acknowledge the excellent technical/logistic help provided by Jasmina Jiménez.

Abbreviations

6-hydroxy-DA: 6-hydroxydopamine

AIMS: Abnormal Involuntary Movements

Ang: Angiotensin

Ang II: Angiotensin II

AT1/2Hets AT1-AT2 Heterodimers

BRET: Bioluminescence Resonance Energy Transfer

BSA: Bovine Serum Albumin

cAMP: Cyclic Adenylic acid

CAN: Candesartan

CGP: CGP-42112A

ChAT: choline acetyltransferase

CNS: central nervous system

CR: Calretinin

Cy3: Cyano 3

DA: Dopamine

DIV: Days In Vitro

DMEM: Dulbecco’s modified Eagle’s medium

DMR: Dynamic Mass Redistribution

DMSO: Dimethyl sulfoxide

FBS: Fetal Bovine Serum

FK: Forskolin

HBSS: Hanks' Balanced Salt Solution

HTRF: Homogeneous Time Resolved Fluorescence

IFN- g: Interferon-g

L-DOPA: Levodopa

LPS: Lipopolysaccharide

MAPK: Mitogen-Activated Protein Kinase

mBU: Milli Bioluminescence resonance energy transfer Units

NaCl: Sodium Chloride

PBS: Phosphate Buffered Saline

PD: Parkinson's disease

PEI PolyEthylenImine

PKA: Protein kinase A

PLA: Proximity ligation assays

PV: Parvalbumin

RAS: Renin-angiotensin system

Rluc: Renilla luciferase

SERCA: Sarco/endoplasmic reticulum Ca^{2+}-ATPase

SN: Substantia nigra

TR-FRET: Time-resolved fluorescence energy transfer

YFP: Yellow Fluorescent Protein

References

1. Abadir, P.M., Periasamy, A., Carey, R.M., Siragy, H.M., 2006. Angiotensin II Type 2 Receptor–Bradykinin B_2 Receptor Functional Heterodimerization. Hypertension 48, 316–322. doi:10.1161/01.HYP.0000228997.88162.a8
2. AbdAlla, S., Lother, H., el Massiery, A., Quitterer, U., 2001. Increased AT1 receptor heterodimers in preeclampsia mediate enhanced angiotensin II responsiveness. Nat. Med. 7, 1003–1009. doi:10.1038/nm0901-1003
3. AbdAlla, S., Lother, H., Quitterer, U., 2000. AT1-receptor heterodimers show enhanced G-protein activation and altered receptor sequestration. Nature 407, 94–98. doi:10.1038/35024095
4. Barki-Harrington, L., Luttrell, L.M., Rockman, H.A., 2003. Dual Inhibition of β-Adrenergic and Angiotensin II Receptors by a Single Antagonist. Circulation 108, 1611–1618. doi:10.1161/01.CIR.0000092166.30360.78
5. Benito, C., Núñez, E., Tolón, R.M., Carrier, E.J., Rábano, A., Hillard, C.J., Romero, J., 2003. Cannabinoid CB2 receptors and fatty acid amide hydrolase are selectively overexpressed in neuritic plaque-associated glia in Alzheimer's disease brains. J. Neurosci. 23, 11136–41.

6. Bennion, D.M., Isenberg, J.D., Harmel, A.T., DeMars, K., Dang, A.N., Jones, C.H., Pignataro, M.E., Graham, J.T., Steckelings, U.M., Alexander, J.C., Febo, M., Krause, E.G., de Kloet, A.D., Candelario-Jalil, E., Sumners, C., 2017. Post-stroke angiotensin II type 2 receptor activation provides long-term neuroprotection in aged rats. PLoS One 12, e0180738. doi:10.1371/journal.pone.0180738
7. Bhat, S.A., Goel, R., Shukla, S., Shukla, R., Hanif, K., 2018. Angiotensin Receptor Blockade by Inhibiting Glial Activation Promotes Hippocampal Neurogenesis Via Activation of Wnt/β-Catenin Signaling in Hypertension. Mol. Neurobiol. 55, 5282–5298. doi:10.1007/s12035-017-0754-5
8. Bhat, S.A., Sood, A., Shukla, R., Hanif, K., 2019. AT2R Activation Prevents Microglia Pro-inflammatory Activation in a NOX-Dependent Manner: Inhibition of PKC Activation and p47 phox Phosphorylation by PP2A. Mol. Neurobiol. 56, 3005–3023. doi:10.1007/s12035-018-1272-9
9. Birkmayer, W., Hornykiewicz, O., 1964. Additional experimental studies on L-DOPA in Parkinson's syndrome and reserpine parkinsonism. Arch. Psychiatr. Nervenkr. 206, 367–81.
10. Cerrato, B.D., Carretero, O.A., Janic, B., Grecco, H.E., Gironacci, M.M., 2016. Heteromerization Between the Bradykinin B2 Receptor and the Angiotensin-(1-7) Mas Receptor: Functional Consequences. Hypertens. (Dallas, Tex. 1979) 68, 1039–48. doi:10.1161/HYPERTENSIONAHA.116.07874
11. Chen, T.-W., Wardill, T.J., Sun, Y., Pulver, S.R., Renninger, S.L., Baohan, A., Schreiter, E.R., Kerr, R.A., Orger, M.B., Jayaraman, V., Looger, L.L., Svoboda, K., Kim, D.S., 2013. Ultrasensitive fluorescent proteins for imaging neuronal activity. Nature 499, 295–300. doi:10.1038/nature12354
12. De Filippis, D., Steardo, A., D'Amico, A., Scuderi, C., Cipriano, M., Esposito, G., Iuvone, T., 2009. Differential Cannabinoid Receptor Expression during Reactive Gliosis: a Possible Implication for a Nonpsychotropic Neuroprotection. Sci. World J. 9, 229–235. doi:10.1100/tsw.2009.31
13. Farré, D., Muñoz, A., Moreno, E., Reyes-Resina, I., Canet-Pons, J., Dopeso-Reyes, I.G., Rico, A.J., Lluís, C., Mallol, J., Navarro, G., Canela, E.I., Cortés, A., Labandeira-García, J.L., Casadó, V., Lanciego, J.L., Franco, R., 2015. Stronger Dopamine D1 Receptor-Mediated Neurotransmission in Dyskinesia. Mol. Neurobiol. 52, 1408–1420. doi:10.1007/s12035-014-8936-x
14. Ferrão, F.M., Lara, L.S., Axelband, F., Dias, J., Carmona, A.K., Reis, R.I., Costa-Neto, C.M., Vieyra, A., Lowe, J., 2012. Exposure of luminal membranes of LLC-PK $_1$ cells to ANG II induces dimerization of AT $_1$ /AT $_2$ receptors to activate SERCA and to promote Ca $^{2+}$ mobilization. Am. J. Physiol. Physiol. 302, F875–F883. doi:10.1152/ajprenal.00381.2011
15. Ferré, S., Baler, R., Bouvier, M., Caron, M.G., Devi, L.A., Durroux, T., Fuxe, K., George, S.R., Javitch, J.A., Lohse, M.J., Mackie, K., Milligan, G., Pfleger, K.D.G., Pin, J.-P., Volkow, N.D., Waldhoer, M., Woods, A.S., Franco, R., 2009. Building a new conceptual framework for receptor heteromers. Nat. Chem. Biol. 5, 131–4. doi:10.1038/nchembio0309-131
16. Franceschi, C., Bonafe, M., Valensin, S., Olivieri, F., De Luca, M., Ottaviani, E., De Benedictis, G., 2006. Inflamm-aging: An Evolutionary Perspective on Immunosenescence. Ann. N. Y. Acad. Sci. 908, 244–254. doi:10.1111/j.1749-6632.2000.tb06651.x
17. Franco, R., Aguinaga, D., Jiménez, J., Lillo, J., Martínez-Pinilla, E., Navarro, G., 2018. Biased receptor functionality versus biased agonism in G-protein-coupled receptors. Biomol. Concepts 9, 143–154.

doi:10.1515/bmc-2018-0013

18. Franco, R., Navarro, G., Rivas Santisteban, R., Awad Alkozi, H., 2019. Potency of melatonin at G-protein-coupled MT1 and MT2 receptors. Available at: osf.io/w7qxh.
19. Garrido-Gil, P., Rodriguez-Perez, A.I., Fernandez-Rodriguez, P., Lanciego, J.L., Labandeira-Garcia, J.L., 2017. Expression of angiotensinogen and receptors for angiotensin and prorenin in the rat and monkey striatal neurons and glial cells. Brain Struct. Funct. 222, 2559–2571. doi:10.1007/s00429-016-1357-z
20. Garrido-Gil, P., Valenzuela, R., Villar-Cheda, B., Lanciego, J.L., Labandeira-Garcia, J.L., 2013. Expression of angiotensinogen and receptors for angiotensin and prorenin in the monkey and human substantia nigra: an intracellular renin-angiotensin system in the nigra. Brain Struct. Funct. 218, 373–88. doi:10.1007/s00429-012-0402-9
21. González-Hernández, M.. D.L., Godínez-Hernández, D., Bobadilla-Lugo, R.A., López-Sánchez, P., 2010. Angiotensin-II type 1 receptor (AT1R) and alpha-1D adrenoceptor form a heterodimer during pregnancy-induced hypertension. Auton. Autacoid Pharmacol. 30, 167–172. doi:10.1111/j.1474-8673.2009.00446.x
22. Grammatopoulos, T.N., Jones, S.M., Ahmadi, F.A., Hoover, B.R., Snell, L.D., Skoch, J., Jhaveri, V. V, Poczobutt, A.M., Weyhenmeyer, J.A., Zawada, W.M., 2007. Angiotensin type 1 receptor antagonist losartan, reduces MPTP-induced degeneration of dopaminergic neurons in substantia nigra. Mol. Neurodegener. 2, 1. doi:10.1186/1750-1326-2-1
23. Hinz, S., Navarro, G., Borroto-Escuela, D., Seibt, B.F., Ammon, C., Filippo, E. De, Danish, A., Lacher, S.K., Červinková, B., Rafehi, M., Fuxe, K., Schiedel, A.C., Franco, R., Müller, C.E., Ammon, Y.C., de Filippo, E., Danish, A., Lacher, S.K., Červinková, B., Rafehi, M., Fuxe, K., Schiedel, A.C., Franco, R., Müller, C.E., Ammon, C., Filippo, E. De, Danish, A., Lacher, S.K., Červinková, B., Rafehi, M., Fuxe, K., Schiedel, A.C., Franco, R., Müller, C.E., 2018. Adenosine A2A receptor ligand recognition and signaling is blocked by A2B receptors. Oncotarget 9, 13593–13611. doi:10.18632/oncotarget.24423
24. Hornykiewicz, O., 2006. The discovery of dopamine deficiency in the parkinsonian brain. J. Neural Transm. Suppl. 70, 9–15. doi:10.1007/978-3-211-45295-0_3
25. Hradsky, J., Mikhaylova, M., Karpova, A., Kreutz, M.R., Zuschratter, W., 2013. Super-resolution microscopy of the neuronal calcium-binding proteins Calneuron-1 and Caldendrin. Methods Mol. Biol. 963, 147–69. doi:10.1007/978-1-62703-230-8_10
26. Jarrott, B., Williams, S.J., 2016. Chronic Brain Inflammation: The Neurochemical Basis for Drugs to Reduce Inflammation. Neurochem. Res. 41, 523–533. doi:10.1007/s11064-015-1661-7
27. Joglar, B., Rodriguez-Pallares, J., Rodriguez-Perez, A.I., Rey, P., Guerra, M.J., Labandeira-Garcia, J.L., 2009. The inflammatory response in the MPTP model of Parkinson's disease is mediated by brain angiotensin: relevance to progression of the disease. J. Neurochem. 109, 656–69. doi:10.1111/j.1471-4159.2009.05999.x
28. Kirik, D., Winkler, C., Björklund, A., 2001. Growth and functional efficacy of intrastriatal nigral transplants depend on the extent of nigrostriatal degeneration. J. Neurosci. 21, 2889–96.

doi:21/8/2889 [pii]

29. Labandeira-Garcia, JL, Rodríguez-Perez, A., Garrido-Gil, P., Rodriguez-Pallares, J., Lanciego, J., Guerra, M.J., 2017. Brain Renin-Angiotensin System and Microglial Polarization: Implications for Aging and Neurodegeneration. Front. Aging Neurosci. 9, 129. doi:10.3389/fnagi.2017.00129
30. Labandeira-Garcia, Jose L, Costa-Besada, M.A., Labandeira, C.M., Villar-Cheda, B., Rodríguez-Perez, A.I., 2017. Insulin-Like Growth Factor-1 and Neuroinflammation. Front. Aging Neurosci. 9, 365. doi:10.3389/fnagi.2017.00365
31. Labandeira-Garcia, J.L., Rodriguez-Pallares, J., Dominguez-Meijide, A., Valenzuela, R., Villar-Cheda, B., Rodríguez-Perez, A.I., 2013. Dopamine-angiotensin interactions in the basal ganglia and their relevance for Parkinson's disease. Mov. Disord. 28, 1337–42. doi:10.1002/mds.25614
32. Law, A.M.K., Yin, J.X.M., Castillo, L., Young, A.I.J., Piggin, C., Rogers, S., Caldon, C.E., Burgess, A., Millar, E.K.A., O'Toole, S.A., Gallego-Ortega, D., Ormandy, C.J., Oakes, S.R., 2017. Andy's Algorithms: new automated digital image analysis pipelines for FIJI. Sci. Rep. 7, 15717. doi:10.1038/s41598-017-15885-6
33. Lee, C.S., Cenci, M.A., Schulzer, M., Björklund, A., 2000. Embryonic ventral mesencephalic grafts improve levodopa-induced dyskinesia in a rat model of Parkinson's disease. Brain 123 (Pt 7, 1365–1379. doi:10.1093/brain/123.7.1365
34. Lee, Y.C., Lin, C.H., Wu, R.M., Lin, J.W., Chang, C.H., Lai, M.S., 2014. Antihypertensive agents and risk of Parkinson's disease: A nationwide cohort study. PLoS One 9, e98961. doi:10.1371/journal.pone.0098961
35. Leonhardt, J., Villela, D.C., Teichmann, A., Münter, L.-M., Mayer, M.C., Mardahl, M., Kirsch, S., Namsolleck, P., Lucht, K., Benz, V., Alenina, N., Daniell, N., Horiuchi, M., Iwai, M., Multhaup, G., Schülein, R., Bader, M., Santos, R.A., Unger, T., Steckelings, U.M., 2017. Evidence for Heterodimerization and Functional Interaction of the Angiotensin Type 2 Receptor and the Receptor MASNovelty and Significance. Hypertension 69, 1128–1135. doi:10.1161/HYPERTENSIONAHA.116.08814
36. Lundblad, M., Andersson, M., Winkler, C., Kirik, D., Wierup, N., Cenci Nilsson, M.A., 2002. Pharmacological validation of behavioural measures of akinesia and dyskinesia in a rat model of Parkinson's disease. Eur. J. Neurosci. 15, 120–132. doi:10.1046/j.0953-816x.2001.01843.x
37. McCarthy, C.A., Vinh, A., Miller, A.A., Hallberg, A., Alterman, M., Callaway, J.K., Widdop, R.E., 2014. Direct Angiotensin AT2 Receptor Stimulation Using a Novel AT2 Receptor Agonist, Compound 21, Evokes Neuroprotection in Conscious Hypertensive Rats. PLoS One 9, e95762. doi:10.1371/journal.pone.0095762
38. Muñoz, A., Garrido-Gil, P., Dominguez-Meijide, A., Labandeira-Garcia, J.L., 2014. Angiotensin type 1 receptor blockage reduces l-dopa-induced dyskinesia in the 6-OHDA model of Parkinson's disease. Involvement of vascular endothelial growth factor and interleukin-1?? Exp. Neurol. 261, 720–732. doi:10.1016/j.expneurol.2014.08.019
39. Navarro, G., Borroto-Escuela, D., Angelats, E., Etayo, I., Reyes-Resina, I., Pulido-Salgado, M., Rodríguez-Pérez, A.A.I., Canela, E.I.E., Saura, J., Lanciego, J.J.L., Labandeira-García, J.L.J., Saura, C.A., Fuxe, K.,

Franco, R., 2018. Receptor-heteromer mediated regulation of endocannabinoid signaling in activated microglia. Relevance for Alzheimer's disease and levo-dopa-induced dyskinesia. Brain. Behav. Immun. 67, 139–151. doi:10.1016/j.bbi.2017.08.015

40. Newell, E.A., Exo, J.L., Verrier, J.D., Jackson, T.C., Gillespie, D.G., Janesko-Feldman, K., Kochanek, P.M., Jackson, E.K., 2015. 2',3'-cAMP, 3'-AMP, 2'-AMP and adenosine inhibit TNF-α and CXCL10 production from activated primary murine microglia via A2A receptors. Brain Res. 1594, 27–35. doi:10.1016/j.brainres.2014.10.059
41. Ohlin, K.E., Sebastianutto, I., Adkins, C.E., Lundblad, C., Lockman, P.R., Cenci, M.A., 2012. Impact of L-DOPA treatment on regional cerebral blood flow and metabolism in the basal ganglia in a rat model of Parkinson's disease. Neuroimage 61, 228–239. doi:10.1016/j.neuroimage.2012.02.066
42. Olanow, C.W., Agid, Y., Mizuno, Y., Albanese, A., Bonuccelli, U., Bonucelli, U., Damier, P., De Yebenes, J., Gershanik, O., Guttman, M., Grandas, F., Hallett, M., Hornykiewicz, O., Jenner, P., Katzenschlager, R., Langston, W.J., LeWitt, P., Melamed, E., Mena, M.A., Michel, P.P., Mytilineou, C., Obeso, J.A., Poewe, W., Quinn, N., Raisman-Vozari, R., Rajput, A.H., Rascol, O., Sampaio, C., Stocchi, F., 2004. Levodopa in the treatment of Parkinson's disease: current controversies. Mov. Disord. 19, 997–1005. doi:10.1002/mds.20243
43. Padia, S.H., Carey, R.M., 2013. AT2 receptors: beneficial counter-regulatory role in cardiovascular and renal function. Pflugers Arch. 465, 99–110. doi:10.1007/s00424-012-1146-3
44. Patel, S., Hussain, T., 2018. Dimerization of AT2 and Mas Receptors in Control of Blood Pressure. Curr. Hypertens. Rep. 20, 1–9. doi:10.1007/s11906-018-0845-3
45. Perez-Lloret, S., Otero-Losada, M., Toblli, J.E., Capani, F., 2017. Renin-angiotensin system as a potential target for new therapeutic approaches in Parkinson's disease. Expert Opin. Investig. Drugs 26, 1163–1173. doi:10.1080/13543784.2017.1371133
46. Phipps, J.A., Vessey, K.A., Brandli, A., Nag, N., Tran, M.X., Jobling, A.I., Fletcher, E.L., 2018. The Role of Angiotensin II/AT1 Receptor Signaling in Regulating Retinal Microglial Activation. Investig. Opthalmology Vis. Sci. 59, 487. doi:10.1167/iovs.17-22416
47. Pinna, A., Bonaventura, J., Farré, D., Sánchez, M., Simola, N., Mallol, J., Lluís, C., Costa, G., Baqi, Y., Müller, C.E., Cortés, A., McCormick, P., Canela, E.I., Martínez-Pinilla, E., Lanciego, J.L., Casadó, V., Armentero, M.-T.T., Franco, R., 2014. l-DOPA disrupts adenosine A2A–cannabinoid CB1–dopamine D2 receptor heteromer cross-talk in the striatum of hemiparkinsonian rats: Biochemical and behavioral studies. Exp. Neurol. 253, 180–191. doi:10.1016/j.expneurol.2013.12.021
48. Porrello, E.R., Pfleger, K.D.G., Seeber, R.M., Qian, H., Oro, C., Abogadie, F., Delbridge, L.M.D., Thomas, W.G., 2011. Heteromerization of angiotensin receptors changes trafficking and arrestin recruitment profiles. Cell. Signal. 23, 1767–1776. doi:10.1016/j.cellsig.2011.06.011
49. Pulido-Salgado, M., Vidal-Taboada, J.M., Garcia Diaz-Barriga, G., Serratosa, J., Valente, T., Castillo, P., Matalonga, J., Straccia, M., Canals, J.M., Valledor, A., Solà, C., Saura, J., 2017. Myeloid C/EBPβ deficiency reshapes microglial gene expression and is protective in experimental autoimmune encephalomyelitis. J. Neuroinflammation 14, 54. doi:10.1186/s12974-017-0834-5

50. Rodriguez-Pallares, J., Rey, P., Parga, J.A., Muñoz, A., Guerra, M.J., Labandeira-Garcia, J.L., 2008. Brain angiotensin enhances dopaminergic cell death via microglial activation and NADPH-derived ROS. Neurobiol. Dis. 31, 58–73. doi:10.1016/j.nbd.2008.03.003
51. Rodriguez-Perez, A.I., Borrajo, A., Rodriguez-Pallares, J., Guerra, M.J., Labandeira-Garcia, J.L., 2015. Interaction between NADPH-oxidase and Rho-kinase in angiotensin II-induced microglial activation. Glia 63, 466–482. doi:10.1002/glia.22765
52. Rodriguez-Perez, A.I., Sucunza, D., Pedrosa, M.A., Garrido-Gil, P., Kulisevsky, J., Lanciego, J.L., Labandeira-Garcia, J.L., 2018. Angiotensin Type 1 Receptor Antagonists Protect Against Alpha-Synuclein-Induced Neuroinflammation and Dopaminergic Neuron Death. Neurotherapeutics 15, 1063–1081. doi:10.1007/s13311-018-0646-z
53. Rozenfeld, R., Gupta, A., Gagnidze, K., Lim, M.P., Gomes, I., Lee-Ramos, D., Nieto, N., Devi, L.A., 2011. AT1R-CB1 R heteromerization reveals a new mechanism for the pathogenic properties of angiotensin II. EMBO J. 30, 2350–2363. doi:10.1038/emboj.2011.139
54. Rubio-Ruíz, M.E., Del Valle-Mondragón, L., Castrejón-Tellez, V., Carreón-Torres, E., Díaz-Díaz, E., Guarner-Lans, V., 2014. Angiotensin II and 1-7 during aging in Metabolic Syndrome rats. Expression of AT1, AT2 and Mas receptors in abdominal white adipose tissue. Peptides 57, 101–108. doi:10.1016/j.peptides.2014.04.021
55. Santos, E.L., Reis, R.I., Silva, R.G., Shimuta, S.I., Pecher, C., Bascands, J.L., Schanstra, J.P., Oliveira, L., Bader, M., Paiva, A.C.M.M., Costa-Neto, C.M., Pesquero, J.B., 2007. Functional rescue of a defective angiotensin II AT1 receptor mutant by the Mas protooncogene. Regul. Pept. 141, 159–167. doi:10.1016/j.regpep.2006.12.030
56. Saura, J., Tusell, J.M., Serratosa, J., 2003. High-Yield Isolation of Murine Microglia by Mild Trypsinization. Glia 44, 183–189. doi:10.1002/glia.10274
57. Schallert T, Kozlowski DA, Humm JL, C.R., 1997. Use-dependent structural events in recovery of function. Adv Neurol 73, 229–238.
58. Siddiquee, K., Hampton, J., McAnally, D., May, L., Smith, L., 2013. The apelin receptor inhibits the angiotensin II type 1 receptor via allosteric trans-inhibition. Br. J. Pharmacol. 168, 1104–1117. doi:10.1111/j.1476-5381.2012.02192.x
59. Steckelings, U.M., Kaschina, E., Unger, T., 2005. The AT2 receptor--a matter of love and hate. Peptides 26, 1401–9. doi:10.1016/j.peptides.2005.03.010
60. Sun, H., Wu, H., Yu, X., Zhang, G., Zhang, R., Zhan, S., Wang, H., Bu, N., Ma, X., Li, Y., 2015. Angiotensin II and its receptor in activated microglia enhanced neuronal loss and cognitive impairment following pilocarpine-induced status epilepticus. Mol. Cell. Neurosci. 65, 58–67. doi:10.1016/j.mcn.2015.02.014
61. Valenzuela, R., Barroso-Chinea, P., Villar-Cheda, B., Joglar, B., Muñoz, A., Lanciego, J.L., Labandeira-Garcia, J.L., 2010. Location of Prorenin Receptors in Primate Substantia Nigra: Effects on Dopaminergic Cell Death. J. Neuropathol. Exp. Neurol. 69, 1130–1142. doi:10.1097/NEN.0b013e3181fa0308

62. Valero-Esquitino, V., Lucht, K., Namsolleck, P., Monnet-Tschudi, F., Stubbe, T., Lucht, F., Liu, M., Ebner, F., Brandt, C., Danyel, L.A., Villela, D.C., Paulis, L., Thoene-Reineke, C., Dahlöf, B., Hallberg, A., Unger, T., Sumners, C., Steckelings, U.M., 2015. Direct angiotensin type 2 receptor (AT_2 R) stimulation attenuates T-cell and microglia activation and prevents demyelination in experimental autoimmune encephalomyelitis in mice. Clin. Sci. 128, 95–109. doi:10.1042/CS20130601
63. Villela, D., Leonhardt, J., Patel, N., Joseph, J., Kirsch, S., Hallberg, A., Unger, T., Bader, M., Santos, R.A., Sumners, C., Steckelings, U.M., 2015. Angiotensin type 2 receptor (AT 2 R) and receptor Mas: a complex liaison. Clin. Sci. 128, 227–234. doi:10.1042/CS20130515
64. Wilson, P.C., Lee, M.-H., Appleton, K.M., El-Shewy, H.M., Morinelli, T.A., Peterson, Y.K., Luttrell, L.M., Jaffa, A.A., 2013. The Arrestin-selective Angiotensin AT_1 Receptor Agonist [Sar^1,Ile^4,Ile^8]-AngII Negatively Regulates Bradykinin B_2 Receptor Signaling via AT_1-B_2 Receptor Heterodimers. J. Biol. Chem. 288, 18872–18884. doi:10.1074/jbc.M113.472381
65. Winkler, C., Kirik, D., Björklund, A., Cenci, M.A., 2002. L-DOPA-induced dyskinesia in the intrastriatal 6-hydroxydopamine model of parkinson's disease: relation to motor and cellular parameters of nigrostriatal function. Neurobiol. Dis. 10, 165–186. doi:10.1006/nbdi.2002.0499

Figures

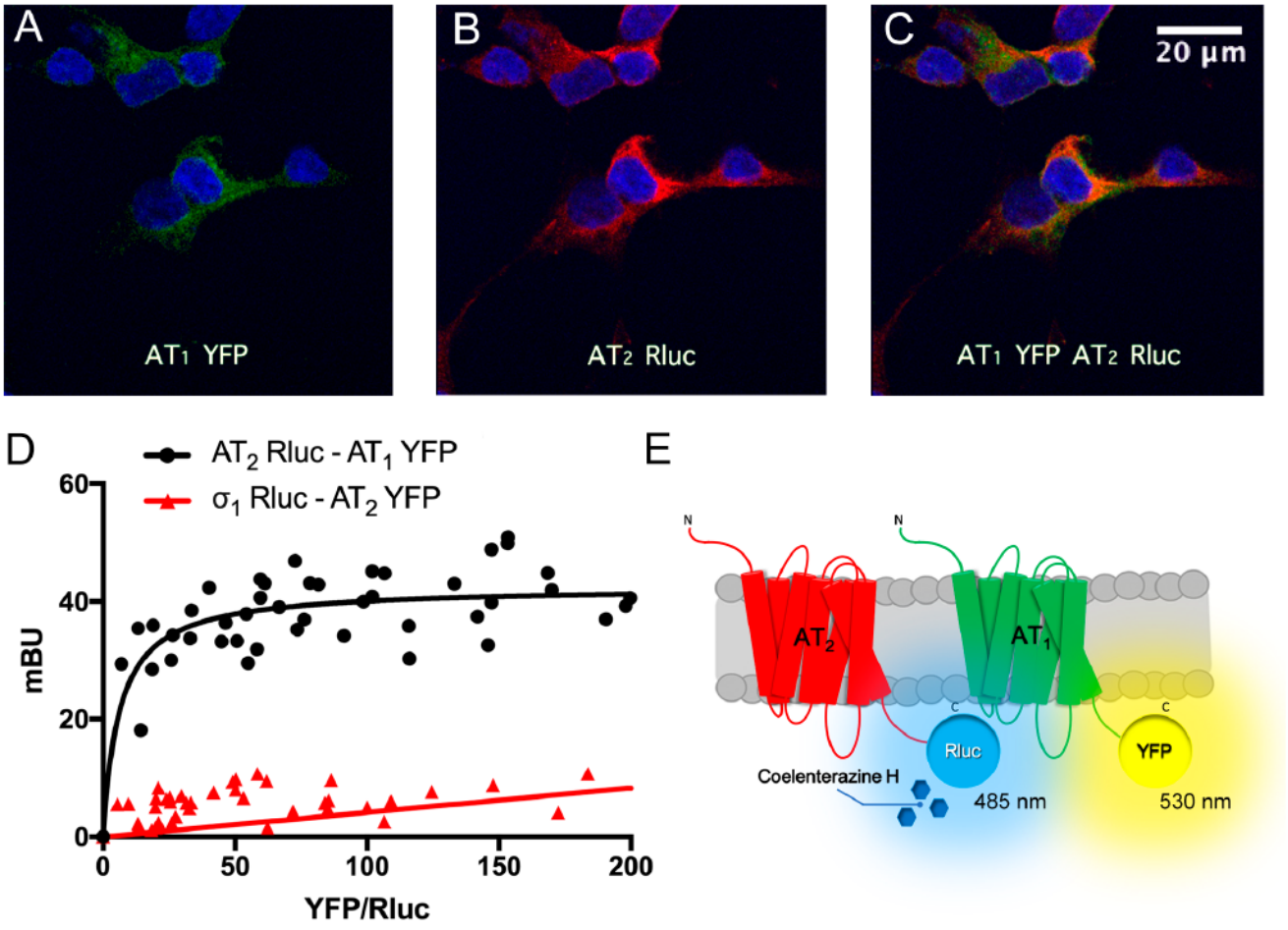

Figure 1

Human AT1 and AT2 receptors interact in a heterologous expression system. Panels A-C: Immunocytochemistry assays were performed in HEK-293T cells expressing AT1R-YFP (1 µg cDNA), which was detected by its own yellow fluorescence (green), and AT2R-Rluc (1 µg cDNA), which was detected by a mouse anti-Rluc antibody and a secondary Cy3 anti-mouse antibody (red). Colocalization is shown in yellow. Cell nuclei were stained with Hoechst (blue). Scale bar: 20 µm. Panel D: BRET assays were performed in HEK-293T cells transfected with a constant amount of cDNA for AT2R-Rluc (0.9 µg) or 1R-Rluc (0.75 µg) (as negative control) and increasing amounts of cDNA for AT1R-YFP (0.5 to 4 µg) or AT2R-YFP (0.1 to 4 µg) (as negative control). Values are the mean ± S.E.M. of 8 independent experiments performed in duplicates. Panel E: Schematic representation of BRET assay: the occurrence of energy transfer depends on the distance between the BRET donor (Rluc) and the BRET acceptor (YFP).

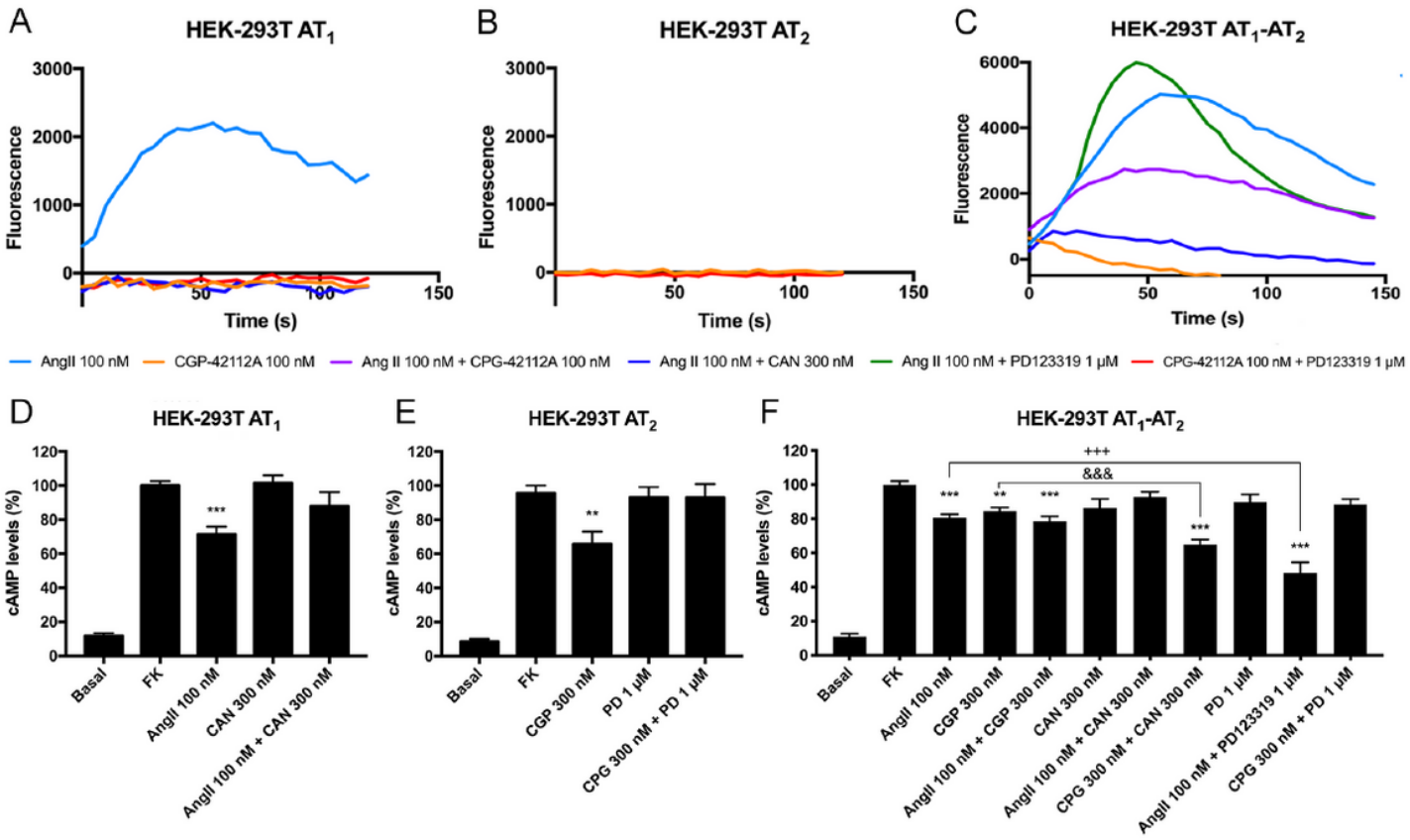

Figure 2

Human AT1 and AT2 receptors interact in a heterologous expression system. Panels A-C: Immunocytochemistry assays were performed in HEK-293T cells expressing AT1R-YFP (1 µg cDNA), which was detected by its own yellow fluorescence (green), and AT2R-Rluc (1 µg cDNA), which was detected by a mouse anti-Rluc antibody and a secondary Cy3 anti-mouse antibody (red). Colocalization is shown in yellow. Cell nuclei were stained with Hoechst (blue). Scale bar: 20 µm. Panel D: BRET assays were performed in HEK-293T cells transfected with a constant amount of cDNA for AT2R-Rluc (0.9 µg) or 1R-Rluc (0.75 µg) (as negative control) and increasing amounts of cDNA for AT1R-YFP (0.5 to 4 µg) or AT2R-YFP (0.1 to 4 µg) (as negative control). Values are the mean ± S.E.M. of 8 independent experiments performed in duplicates. Panel E: Schematic representation of BRET assay: the occurrence of energy transfer depends on the distance between the BRET donor (Rluc) and the BRET acceptor (YFP).

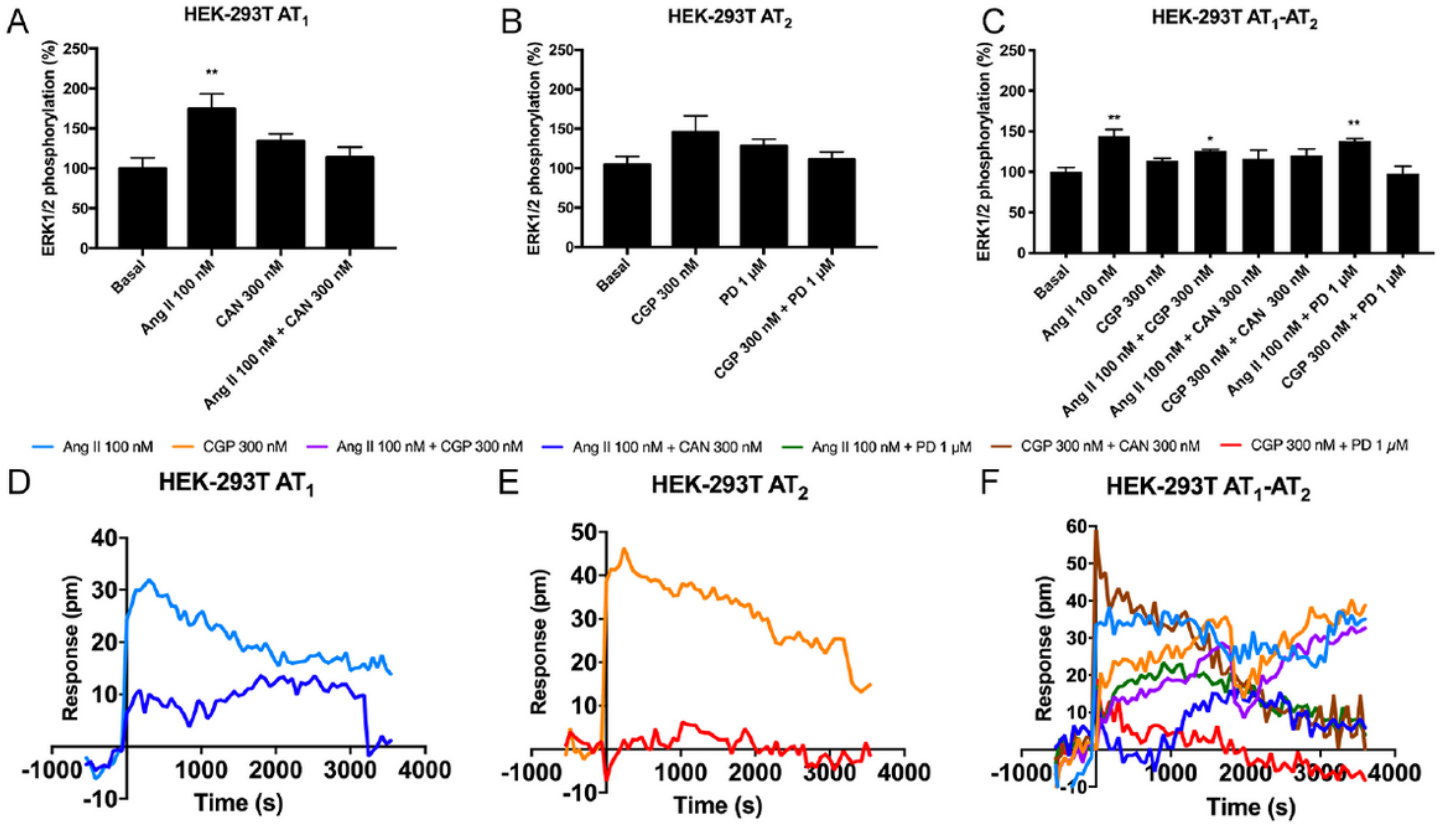

Figure 3

Functional characterization of AT1R-AT2R heteromer in HEK-293T cells. HEK-293T cells were transfected with cDNAs for AT1R (1 µg) and/or AT2R (1 µg). Cells were pretreated (15 min) with selective receptor antagonists (300 nM candesartan for AT1R or 1 µM PD123319 for AT2R receptors) and subsequently treated with selective agonists (100 nM angiotensin II for AT1R and 300 nM CGP-42112A for AT2R receptors). Panels A-C: ERK1/2 phosphorylation was analyzed using an AlphaScreen®SureFire® kit (Perkin Elmer). Values are the mean ± S.E.M. of 5 independent experiments performed in duplicates. One-way ANOVA followed by Bonferroni's multiple comparison post-hoc test were used for statistical analysis. Signaling output was the dependent variable and the different treatments were the independent variables (*$p < 0.05$, **$p < 0.01$, ***$p < 0.001$; versus vehicle treatment (basal)). Panels D-F: DMR tracings represent the picometer-shifts of reflected light wavelength over time. Values are the mean ± S.E.M. 8 independent experiments performed in triplicates.

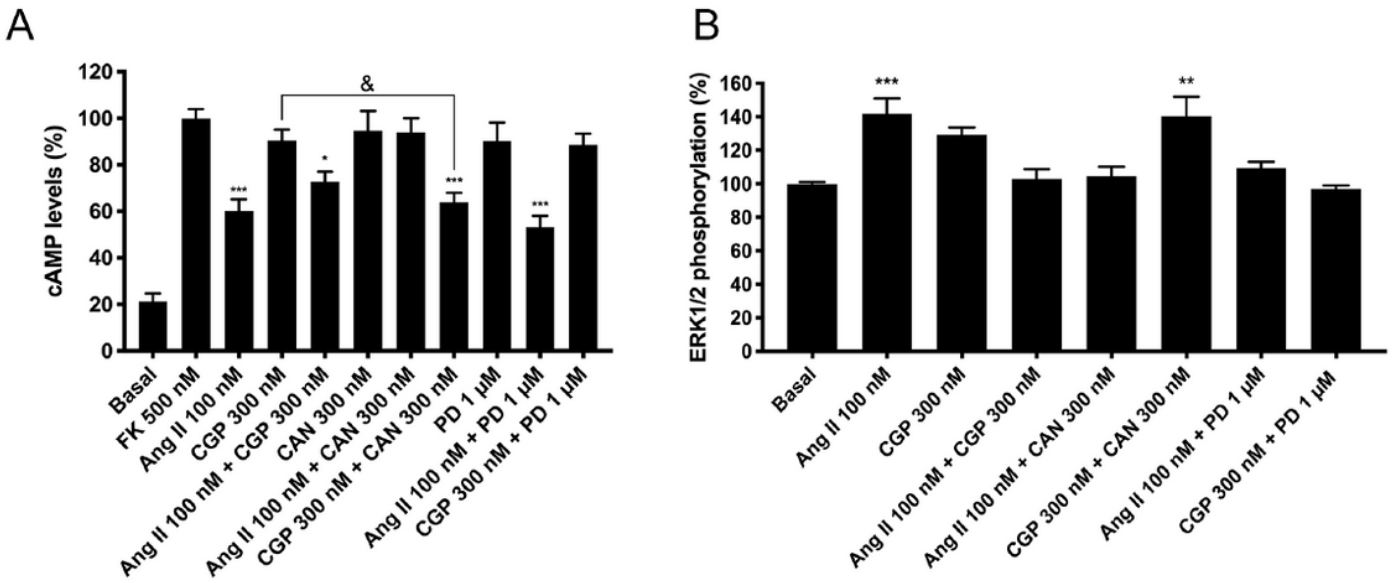

Figure 4

AT1R-AT2R heteromer functionality in primary cultures of striatal neurons. For cAMP (A) or ERK1/2 phosphorylation (B), cells were pretreated (15 min) with selective receptor antagonists (300 nM candesartan for AT1R or 1 µM PD123319 for AT2R) and subsequently treated with selective agonists (100 nM angiotensin II for AT1R and/or 300 nM CGP-42112A for AT2R). Values are the mean ± S.E.M. of 5 independent experiments performed in triplicates. One-way ANOVA followed by Bonferroni's multiple comparison post-hoc test were used for statistical analysis. Signaling output was the dependent variable and the different treatments were the independent variables. (&p < 0.05 CGP-42112A treatment in cAMP determinations; and *p < 0.05, **p < 0.01, ***p < 0.001 versus forskolin treatment in cAMP determinations or versus vehicle treatment (basal) in pERK determinations).

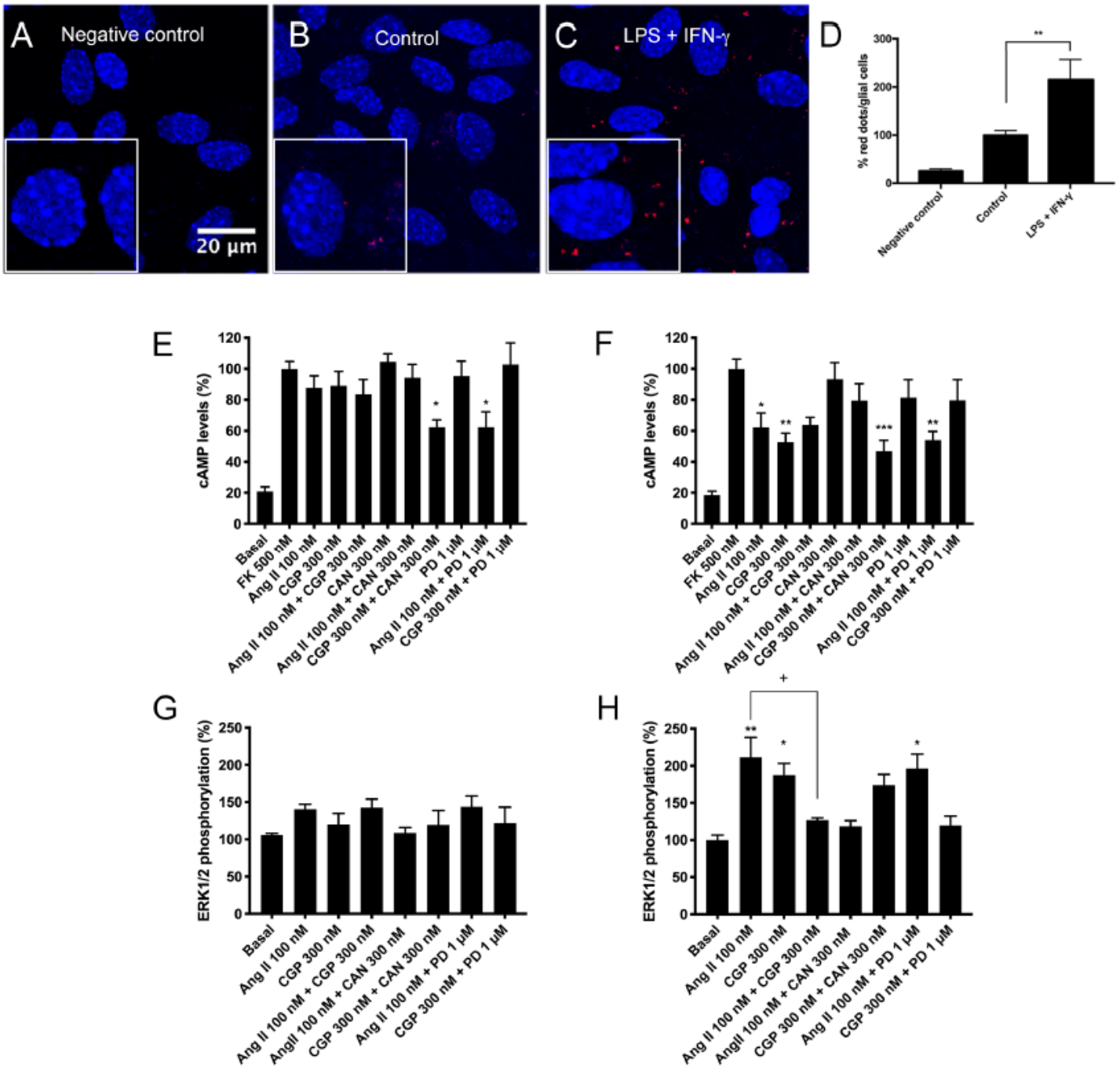

Figure 5

AT1R-AT2R heteromer functionality in microglial primary cultures treated with LPS and IFN-γ. Panels A-C: Expression of AT1R/AT2R heteromers in primary microglial cultures were determined by PLA, which was performed using specific primary antibodies against AT1 and AT2 receptors (Confocal microscopy images (stacks of 3 consecutive planes) show heteroreceptor complexes as red clusters and Hoechst-stained nuclei (blue). Scale bar: 20 µm. Panel D: Bar graph showing the percentage of red dots/cell respect non-treated cells; mean ± S.E.M of counts in 5-7 different fields (n=5; **p < 0.01; Student's t test versus the control condition). Panels E-F: Microglial cultures were incubated for 48 h in the absence (left)

or in the presence (right) of 1 μM LPS and 200 U/mL IFN-. Microglial cells were pretreated (15 min) with selective receptor antagonists (300 nM candesartan for AT1R or 1 μM PD123319 for AT2R receptors) and subsequently with the specific agonists (100 nM Angiotensin II for AT1R and 300 nM CGP-42112A for AT2R receptors). cAMP (E) and ERK1/2 phosphorylation (F) were subsequently measured. Values are the mean ± S.E.M. of 5 independent experiments performed in triplicates. One-way ANOVA followed by Bonferroni's multiple comparison post-hoc test were used for statistical analysis. Signaling output was the dependent variable and the different treatments were the independent variables. (+p < 0.05 versus Ang II treatment in pERK determinations; and *p < 0.05, **p < 0.01, ***p < 0.001; versus forskolin treatment in cAMP measurements or versus vehicle treatment (basal) in pERK measurements).

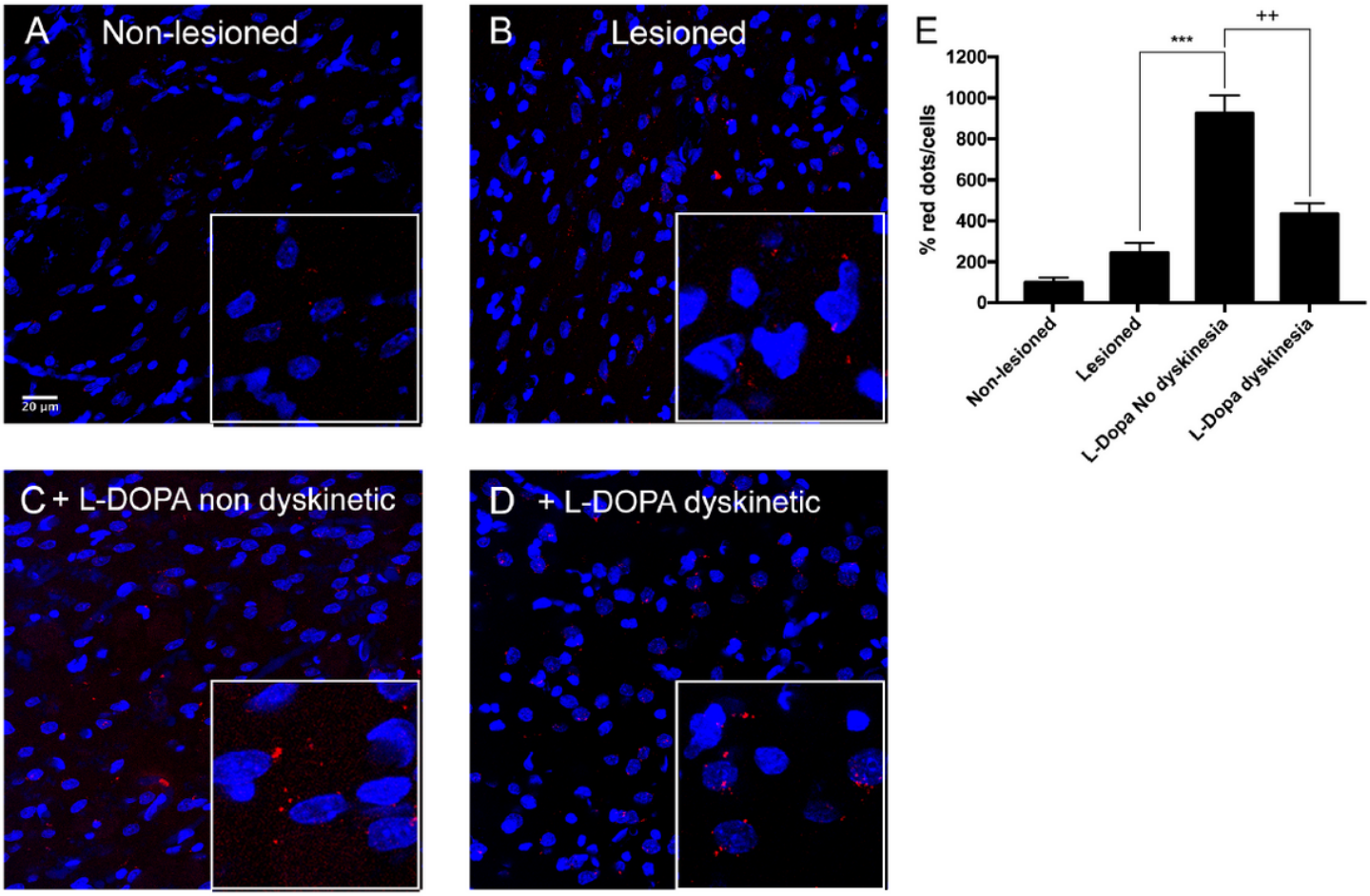

Figure 6

AT1R-AT2R heteromer expression in brain striatal sections of Parkinson's Disease (PD) rat model. Panels A-D. PLA assays in striatal sections from the 6-hydroxy-dopamine PD rat model, non-lesioned (A), lesioned (B) and lesioned plus chronically treated with L-DOPA and either lacking (C) or displaying (D) dyskinesias. Confocal microscopy images (stacks of 3 consecutive planes) show heteroreceptor complexes as red clusters and Hoechst-stained nuclei (blue). Scale bar: 20 μm. Panel E: Bar graph showing the percentage of red dots/cell. Data are the mean S.E.M . of counts in 9-12 different fields per animal (n=4 per group). One-way ANOVA followed by Bonferroni's post-hoc multiple comparison tests

was used to compare the red dots/cell values. The number of clusters (r) was the dependent variable and the four animal groups treatments were independent variables- (***p < 0.001; versus lesioned condition, ++p < 0.01; versus L-DOPA non-dyskinesia condition).

Supplementary Files

This is a list of supplementary files associated with this preprint. Click to download.

- SupplementaryMaterial.docx
- formula.docx